Journal of Solid State Chemistry **158,** 227–235 (2001)
doi:10.1006/jssc.2001.9096, available online at http://www.idealibrary.com on IDEAL®

Magnetotransport and Heat Capacity in Ternary Compounds $U_3M_2M'_3$, M = Al, Ga; M' = Si, Ge

R. Troć,* P. Rogl,† V. H. Tran*, and A. Czopnik*

*W. Trzebiatowski Institute of Low Temperature and Structure Research, Polish Academy of Sciences, P.O. Box 1410, 50-950 Wrocław, Poland; and †Institut für Physikalische Chemie, Universität Wien, Währinger Straße 42, A-1090 Wien, Austria

Received September 14, 2000; in revised form January 3, 2001; accepted January 19, 2001; published online March 27, 2001

We report detailed studies of magnetization, electrical resistivity, magnetoresistivity, and heat capacity performed on the novel family of intermetallic compounds $U_3M_2M'_3$, (M = Al, Ga, and M' = Si, Ge). The present measurements support the earlier conclusions about the ferrimagnetic properties of silicides and ferromagnetic properties of germanides. The resistivity for both compounds $U_3\{Al, Ga\}_2Si_3$ exhibits below T_C a pronounced maximum observed for the first time in an actinoid-ferrimagnet, probably caused by (a) the reduction of the number of effective conduction carriers or (b) a SDW-type of spin-disorder scattering of electrons. Both low-temperature resistivity (except for $U_3Ga_2Si_3$) and heat capacity may be described by a T-dependence involving a small gap Δ on the order of 30–50 K in the magnon dispersion. The C_p/T values at 2 K are enhanced and point to a medium–heavy fermion character of all these ternaries. Magnetoresistance for ferrimagnetic $U_3\{Al, Ga\}_2Si_3$ is rather small but positive in correspondence of antiferromagnetic interactions. In correspondence to the ferromagnetic materials, negative magnetoresistance is encountered for $U_3\{Al, Ga\}_2Ge_3$. Specific features in the temperature dependence of magnetoresistivity $\Delta\rho/\rho$ at various fields confirm the sinusoidal modulation of the magnetic structure for $U_3Al_2Ge_3$ between 40 and 60 K. Also, such data for $U_3Ga_2Ge_3$ present strong indications for a similar magnetic modulation between 63 and 93 K, yet to be discovered by neutron diffraction experiments. In addition, the transition at 63 K is furthermore well resolved in the specific heat data of $U_3Ga_2Ge_3$.

Key Words: **magnetoresistivity; heat capacity; ternary uranium compounds.**

1. INTRODUCTION

The crystal structure and magnetic studies of the intermetallic compounds $U_3M_2M'_3$, where M = Al, Ga, and M' = Si, Ge, have shown interesting features as a function of temperature and applied magnetic fields (1–4). These compounds crystallize with the $U_3Ga_2Ge_3$-structure type (space group $I4$) classified as a low-symmetry derivative of the anti-Cr_5B_3-type (2).

The first magnetic investigation of these phases, made on polycrystalline samples, revealed that all compounds exhibit ferromagnetic ordering, with higher Curie temperatures and saturation moments per uranium atom for germanides than for silicides, though the U–U distances in both groups of compounds are almost the same (≈ 0.35 nm) (1). This feature can rather be related to the difference in the uranium-ligand hybridization effects, than to the U–U distances, which concerns almost all the actinide intermetallic compounds.

The crystal and magnetic structures of the $U_3M_2M'_3$ intermetallics have also been studied by means of neutron powder diffractometry (2, 3). Backed by X-ray single-crystal data (2), these investigations confirmed the almost fully ordered distribution of M and M' atoms at the 8c sites. Besides, the temporal magnetic structures for all four compounds were established (3) on polycrystalline samples. In both silicides the moments of the three uranium atoms U1, U2, and U3, located at the $2a_1$, $2a_2$, and 8c sites, respectively, were assumed to be aligned in the basal plane, but their magnitudes were different. Moreover, the moments at the sites $2a_1$ and 8c are parallel while those at the $2a_2$ site are antiparallel, which yields an overall ferrimagnetic order. The net values are 0.95 and 1.24 μ_B/U atom for the Al- and Ga-containing silicides, respectively (3).

In contrast to the silicides, the magnetic order for both germanides is ferromagnetic, because the moments of the U2 atoms at the $2a_2$ sites with high probability are not magnetically ordered (3). For these germanides the moments of U1 and U3 atoms, though having different magnitudes, are also assumed to be aligned in the basal plane, and their average values are 1.48 and 2.32 μ_B/U atom for the Al- and Ga-containing germanides, respectively (3). In addition, weak satellite reflections in the neutron diffraction diagrams of $U_3Al_2Ge_3$, observed between 40 K and T_C, indicated a sinusoidally modulated uranium moment in the direction of the c axis, with a wave vector $\mathbf{k} = [0, 0, 0.076]$ (3).

In the present work, we supply data on the electrical resistivity, magnetoresistivity, and heat capacity, which are

0022-4596/01 $35.00

TABLE 1
Structural and Magnetic Parameters for the Ternary Compounds of General Formula $U_3(Al, Ga)_2(Si, Ge)_3$

Compound	Lattice parameters (nm)		Magn. order	T_t (K)	T_C (K)	Magnetic moment M_a (μ_B)(2, 3)			Resulting mom./U at.
	a	c				$U_1(2a_1)$	$U_2(2a_2)$	$U_3(8c)$	
$U_3Al_2Si_3$	0.7629(1)	1.0850(1)	Ferri.	—	38	1.13(3)	− 0.46(4)	1.26(3)	0.95
$U_3Ga_2Si_3$	0.7643(1)	1.0838(1)	Ferri.	—	60	1.29(3)	− 0.73(4)	1.72(3)	1.24
$U_3Al_2Ge_3$	0.7749(1)	1.1037(1)	Ferro.	40	60	1.10(5)	—	1.57(2)	1.48
						$M_c = 1.9(1)$	—	$M_c = 1.13(7)$	sine wave
$U_3Ga_2Ge_3$	0.7749(1)	1.1036(1)	Ferro.	63		2.12(9)	—	2.37(4)	2.32
					93	?	?	?	?

supposed to provide additional resolution on the transitions occurring in these systems. We have also extended measurements of the magnetic behavior of these compounds at lower magnetic fields and in other temperature ranges as compared to those reported previously (1).

2. EXPERIMENTAL DETAILS

All four samples with nominal compositions $U_3\{Al,Ga\}_2\{Si,Ge\}_3$ were prepared by arc melting the constituent elements with stoichiometric compositions under argon atmosphere. Other details of synthesis were given in (1). All samples were checked by X-rays to be single phase. It should be noted that the samples studied here have not been annealed. The obtained lattice parameters are given in Table 1. As in earlier procedures we did not find any differences in lattice parameters and susceptibility, but only some small variation in the ordering temperatures after annealing.

Magnetic measurements were carried out in the 1.7–300 K range and in fields up to 5.5 T, employing a SQUID magnetometer. The electrical resistivity and magnetoresistivity (MR) were measured with a standard DC-four probe method at temperatures ranging from 4.2 to 300 K and from 4.2 to 100 K, respectively. The temperature runs were performed first in zero-field, in some occasions several times, and then at a constant field of 8 T. Other runs were made at a constant temperature and in applied magnetic fields varying up to 8 T. In all these cases the sample was cooled to 4.2 K and data were recorded by increasing the magnetic field.

Heat capacity measurements were made between 2 and 70 K by a semiadiabatic method.

3. EXPERIMENTAL RESULTS AND DISCUSSION

3.1. $U_3\{Al, Ga\}_2Si_3$

In the present study, we find on the polycrystalline samples that the magnetization taken at 1.7 K for both these systems behaves in a similar way, i.e., it is almost negligible up to about 0.5 T and then increases sharply to show a tendency to saturation in fields above about 3 T (see Fig. 1). The magnetization values of 0.53 and 0.60 μ_B/U atom for the Al- and Ga-containing silicides, evaluated at 5.5 T, are in general agreement with the respective values found in a previous report (1). However, these values are approximately only half of those found in the neutron diffraction investigations (2, 3). Such findings are thus expected for a uniaxial system, to which these tetragonal symmetry compounds belong.

The presence of the critical field B_{cr} in the field range mentioned above was also observed in isothermal magnetization measurements at 5 K up to 5 T performed on a single

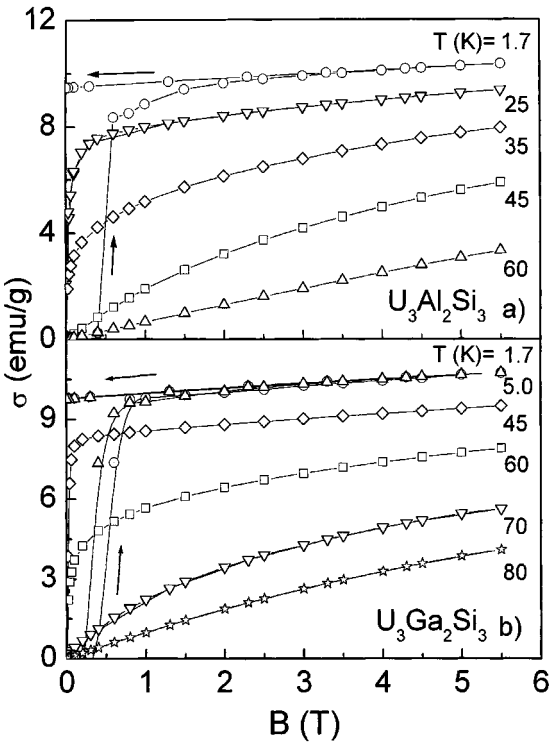

FIG. 1. Magnetization as a function of an applied magnetic field at various temperatures for polycrystalline samples of (a) $U_3Al_2Si_3$ and (b) $U_3Ga_2Si_3$. Note that for the latter compound circles and triangles correspond to the magnetization curves taken at 1.7 and 5 K, respectively.

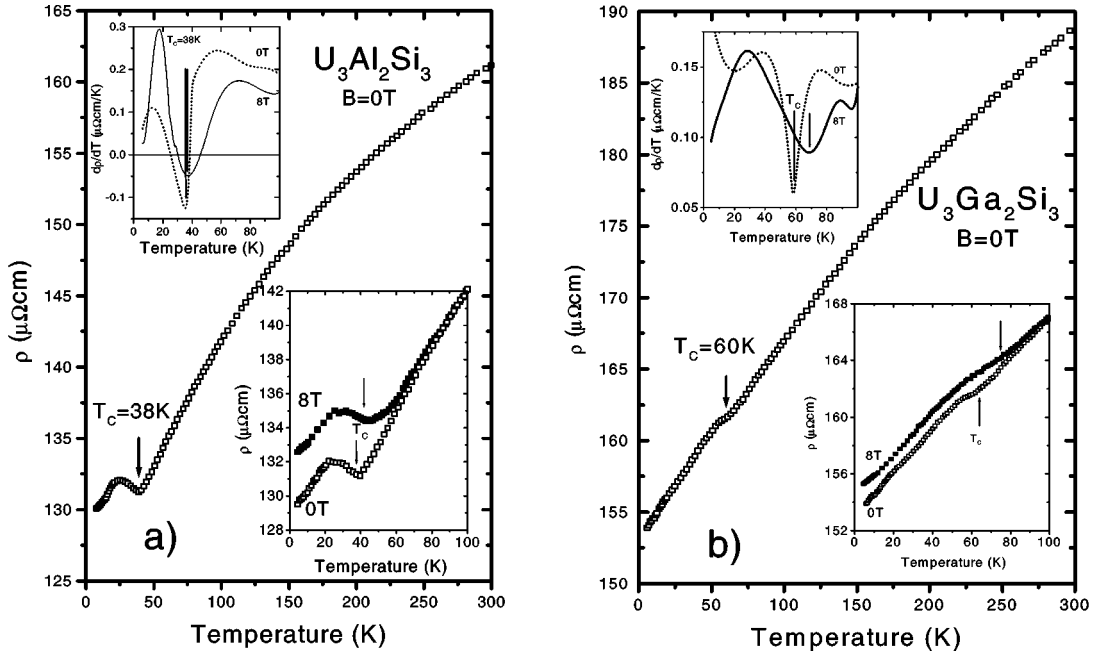

FIG. 2. Temperature dependence of the electrical resistivity for (a) $U_3Al_2Si_3$ and (b) $U_3Ga_2Si_3$. The upper inset shows the temperature derivative of the resistivity. The lower inset shows the low-temperature behavior of the resistivity at zero (open points) and 8 T (solid points).

crystal of $U_3Al_2Si_3$ (4). Its magnetization easy axis **a** was aligned parallel to the direction of the applied field. For both poly- and single crystalline samples of $U_3Al_2Si_3$, the isothermal magnetization above the jump at B_{cr} increases slightly with a further increase of the applied magnetic field; however, it does not completely saturate in a field of 5.5 T. The presence of the magnetocrystalline anisotropy effect is well seen in the low-field magnetization. There is a strong dependence on the history of cooling the samples. For these two Al- and Ga- compounds mentioned above the zero-field cooled (ZFC) magnetization is first constant up to about 15 K, then jumps, goes through a very broad maximum, and finally falls down sharply around T_C (not shown here). As one could expect, the field cooled (FC) magnetization increases smoothly with decreasing temperature for all temperatures below T_C. The temperature dependences of the inverse susceptibility above T_C for both compounds, being strongly curvilinear toward the temperature axis, yielded the same magnetic parameters as previously reported (1)

The temperature dependences of the electrical resistivity ρ of both silicides are presented in Figs. 2a and 2b. In these two cases, ρ increases in a convex way above the corresponding T_C's, which are marked by arrows in these figures. This convexity manifests itself from two contributions: (a) from a high contribution of a phonon-type scattering of electrons and/or (b) the presence of magnetic fluctuations or crystal electrical field effects. Thus such a behavior gives evidence about the absence of a Kondo effect in these compounds. A similar evolution of the resistivity with temperature above the ordering temperature T_N has recently been observed, e.g., in $UPd_{4.5}In_{0.5}$ (5).

Furthermore, the resistivity just below the corresponding Curie temperatures, T_C's, goes through a more ($U_3Al_2Si_3$) or less ($U_3Ga_2Si_3$) pronounced maximum, as is sometimes observed for some intermetallic uranium antiferromagnets, e.g., for UCu_5 (6) and $U_3Cu_4Si_4$ (7). However, the most pronounced maximum in $\rho(T)$ below T_N has as yet been found for semimetallic USb (8). As to our knowledge, such a maximum in the case of a ferrimagnet belonging to the actinide family of compounds has been observed for the first time. It seems that two competing mechanisms are involved here. One is connected with the reduction of a number of effective conduction carriers due to the reconstruction of the Fermi surface by setting in a magnetic order (forming a superzone gap), which causes the increase in the ρ values. The other mechanism is the spin-disorder scattering of electrons, which decreases ρ with lowering temperature (9). This behavior can also be characterized as a spin density wave (SDW)-like transition in which a gap in the electronic excitation spectrum is developed for certain regions in reciprocal space (10).

The influence of an external field on $\rho(T)$ is shown in the lower insets of Figs. 2a and 2b for the Al- and Ga-containing silicides, respectively. For both these cases the 8 T applied field acts to increase slightly the corresponding Curie temperatures, which is well seen on the upper insets of the above

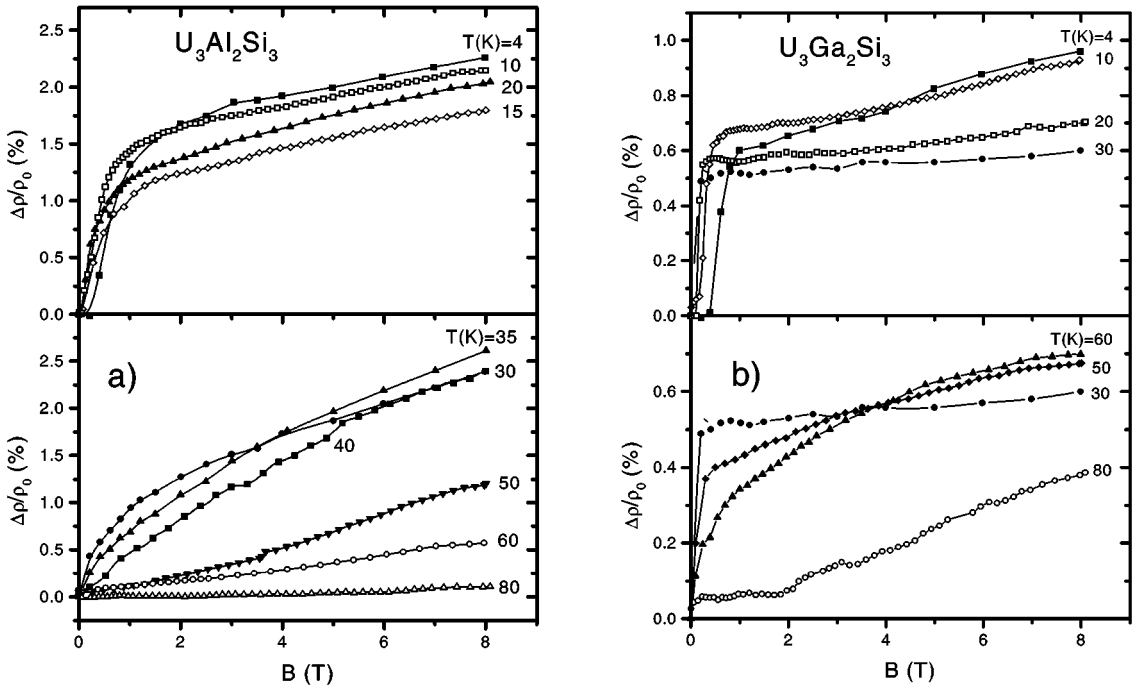

FIG. 3. The magnetoresistivity $\Delta\rho/\rho_o$ as a function of an applied magnetic field for (a) $U_3Al_2Si_3$ and (b) $U_3Ga_2Si_3$ at various temperatures.

mentioned figures, where the temperature derivative of the resistivity is plotted against the temperature for zero and 8 T applied field. The T_C's are marked in these insets by the respective arrows and are represented as a deep minimum in the $d\rho(T)/dT$ versus temperature curves.

Considering the occurrence of the maximum in $\rho(T)$ just below T_C for both compounds, one sees in the lower insets of Figs. 2a and 2b, that the resistivities around this maximum have higher values at 8 T than those taken in zero-magnetic field. This observation is quite opposite to that usually found for a normal antiferromagnet among uranium compounds, where such a "bump" behaviour of the resistivity is usually depressed by the aplied magnetic field (see for example Ref. (5)).

Figures 3a and 3b present the field dependent MR up to 8 T for $U_3Al_2Si_3$ and $U_3Ga_2Si_3$, respectively. MR is defined as $\Delta\rho/\rho_0 = \rho(B) - \rho(0)/\rho(0)$. Comparing the above two figures with Figs. 1a and 1b, one sees that MR and magnetization as a function of the applied magnetic field, show a large similarity for both compounds. As does the magnetization, also the $\Delta\rho/\rho_o$ vs B curves indicate the presence of B_{cr} at low temperatures and the tendency for saturation at higher applied magnetic fields. Subsequently, in Fig. 4, the $\Delta\rho/\rho_o$ values obtained at 8 T are plotted against temperature (solid circles) together with the experimental points obtained from continuous measurements of the temperature dependence of MR taken as a difference between the 8 T and zero-field curves (open points). It is clear from this figure that all these data form two singular functions for both compounds. Although the absolute values of the magnetoresistivity are rather small and differ slightly among themselves (lower values for $U_3Ga_2Si_3$), nevertheless they are all positive like for an antiferromagnet (11). Both these ferrimagnetic compounds exhibit a similar temperature

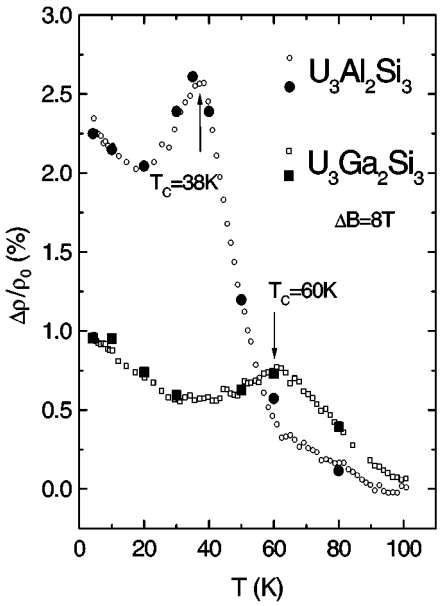

FIG. 4. Magnetoresistivity $\Delta\rho/\rho_o$ as a function of temperature for $U_3Al_2Si_3$ (open and solid circles) and $U_3Ga_2Si_3$ (open and solid squares). The solid points are the data obtained for both compounds from Fig. 3 at 8 T.

shaped dependence of MR, i.e., $\Delta\rho/\rho_o$ first goes through a shallow minimum and then through a broad maximum at the corresponding T_C's. Above the temperature of this maximum, MR shows a long tail, probably due to short-range magnetic order, which spreads out to about 100 K, where MR for both silicides approaches approximately zero. Because of the temperature limitation of our measurements, we can only speculate that the normal negative αB^2 behavior in the paramagnetic state is probably reached far away from the Curie temperature. It should be noted that both compounds show no sign of a Kondo effect. Generally, the observed MR behavior agrees with that expected for the antiferromagnetic state, since the magnetic field causes the instability of magnetic moments oriented antiparallel to its application, which leads to an increase of the resistivity. However, we deal here with a ferrimagnet in which two unequal moments are parallel, whereas the third moment with a different magnitude is oriented antiparallel. Hence, the positive absolute values of MR in these silicides are rather small compared to those in normal antiferromagnets (see for example Ref. (12)). Nevertheless this interesting observation may indicate that the antiferromagnetic interactions are dominant in these compounds.

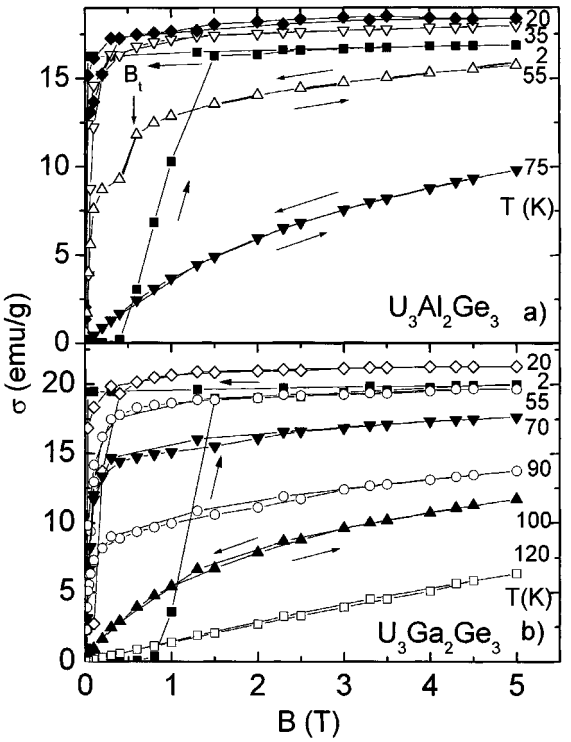

FIG. 5. Magnetization as a function of an applied magnetic field at various temperatures for polycrystalline samples of (a) $U_3Al_2Ge_3$ and (b) $U_3Ga_2Ge_3$.

3.2. $U_3\{Al, Ga\}_2, Ge_3$

In contrast to the isotypic silicides, the two germanides are ferromagnets, as neutron diffraction studies indicated (2, 3). The Curie temperatures are rather high and amount to 60 and 93 K for the Al- and Ga-containing germanides, respectively. Similar to the low-field temperature dependence of the magnetization observed in silicides, the dependence for $U_3Ga_2Ge_3$ indicates a large irreversibility in the ZFC and FC thermal magnetizations (not shown here). Figures 5a and 5b show the magnetization curves vs applied magnetic field curves for the $U_3Al_2Ge_3$ and $U_3Ga_2Ge_3$ polycrystalline samples, respectively, taken at various temperatures. The 2K-curve for the former compound follows almost exactly the behavior of that found at 5 K for a single-crystalline sample of this compound (4). Namely, the magnetization first jumps above B_{cr}, which at 2 K is close to about 0.5 and 1 T, for the aluminide and gallide ternaries, respectively, and then at a field of about 1.5 T both show a complete saturation to the respective values of 1.0 and 1.3 μ_B. It is interesting to note that the saturation magnetization at 20 K for both these ternaries is higher than that at 2 K. These values are about 60–70% of the average magnetic moments evaluated from the neutron diffraction experiment. This is evidence of some preference in the grain arrangement along the magnetization easy axis. In addition, a small jump in the magnetization at about $B_t = 0.5$ T in the isothermal curve of 55 K (see Fig. 5a), being well reproducible with increasing and decreasing magnetic fields, is observed for $U_3Al_2Ge_3$ in the temperature region of the stability of its sine-wave magnetic structure. The susceptibility in the paramagnetic state for the aluminide and gallide germanides follows exactly the Curie–Weiss law, exactly with the same magnetic parameters as given in Ref. (1).

The temperature variations of the electrical resistivity for the Al- and Ga-containing germanides are shown in Figs. 6a and 6b. The overall temperature behavior of both these ferromagnetic germanides is slightly different than that for the silicides described above. For both germanides there is a distinct change of slope in $\rho(T)$ at the corresponding Curie temperatures and an almost linear variation above this temperature. However, the problem arises in the data obtained below T_C. It turns out that the zero-field $\rho(T)$ curve taken in the temperature range of the ordered state was not reproducible and several runs were needed to obtain finally a full reproducibility. In the lower insets of Figs. 6a and 6b we present the first (curve 1) and last (curve 2 or 3) runs of $\rho(T)$ taken in zero-field. Nevertheless, these curves, independent of the number of runs were made, clearly show at T_t an additional transition revealed by a small "knee" in $\rho(T)$. In the case of $U_3Al_2Ge_3$, a situation seems to be clear because the transition to a sine-wave modulated structure along the c axis has been revealed above $T_t \approx 40$ K by neutron powder diffraction (3). The low-temperature dependencies of the zero-field resistivity for both compounds were first fitted to

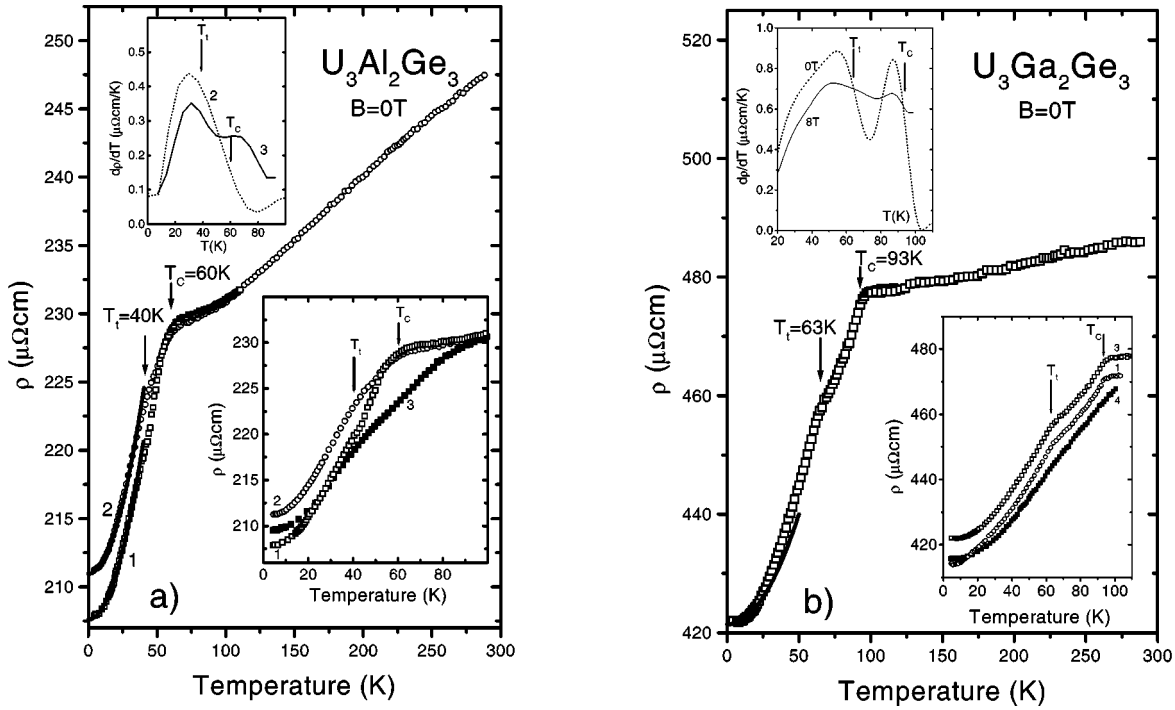

FIG. 6. Temperature dependence of the electrical resistivity for (a) $U_3Al_2Ge_3$ and (b) $U_3Ga_2Ge_3$. The upper inset shows the temperature derivative of the resistivity. The lower inset shows the low temperature behavior of the resistivity at zero (open points) and 8 T (solid points). At low temperatures, the T^2 dependence is marked by a solid line.

the equation $\rho(T) = \rho_0 + AT^2$. For $U_3Al_2Ge_3$ the constant ρ_0 and A, determined from fitting to curves (1) and (2), are very close to each other and their average values are 210(5) μΩ cm and 0.0082(3) μΩ cm^2/K^{-2}, respectively. The corresponding parameters found for $U_3Ga_2Ge_3$ are 421(2) μΩ cm and 0.0087(5) μΩ cm^2/K^{-2}, but apply to a more limited temperature region below 20 K as compared to about 40 K for the aluminide. However, on the basis of the heat capacity analysis, as will be discussed below, one should obtain a better agreement by taking into account an activation behavior. For all the compounds studied, except for $U_3Ga_2Si_3$, the temperature dependence of the resistivity could also be fitted taking into account electron–magnon scattering:

$$\rho_{\mathrm{Ferro}}(T) = \rho_{\mathrm{o}} + BT + CT^2 \exp(-\Delta/T).$$

Here B and C are constants and Δ is a gap in the spin–wave spectrum. The resulting values of Δ, obtained from the fitting of the experimental data to the above expression in the ranges of temperature 4.2–20 K and 4.2–40 K for $U_3Al_2Si_3$ and $U_3\{Al, Ga\}_2, Ge_3$, respectively, are all around 29 (2) K. To get more precise fitting parameters in the resistivity measurements one needs to go to considerably lower temperatures than those available in this work.

The magnetic-field dependent MR for $U_3Al_2Ge_3$ and $U_3Ga_2Ge_3$ is displayed in Figs. 7a and 7b. In contrast to the silicides, MR here is negative for all the temperatures studied, i.e., from 4.2 to 100 K. It is well known that a negative MR is characteristic either for ferromagnets due to decreasing the spin-disorder resistivity by the applied magnetic field, or of the systems, where there exist many body electron–electron interactions, such as spin-fluctuations or Kondo-like effect (12). As Fig. 7a indicates, in the temperature range of the existence of a collinear ferromagnetic structure up to 40 K, MR behaves in different way than in the temperature range where the sine-wave modulated structure is stable. For the former case, MR shows first a low-field minimum, being not understood at present (Fig. 7a, top panel) and then behaves almost linearly with increasing magnetic field strength up to 8 T. In contrast to that, the $\Delta\rho/\rho_o$ vs B curves at temperatures, where the sine-wave modulated structure is stable, i.e. between 40–60 K (Fig. 7a, bottom panel), show rather a curvilinear $-AB^n$ ($n \approx 1/2$) character with a weak tendency to saturation at higher fields (Fig. 7b). In the paramagnetic state MR behaves in a typical way, i.e. it closely follows a negative αB^2 variation.

In Fig. 8, we plotted the $\Delta\rho/\rho_o$ vs T dependence for $U_3Al_2Ge_3$, taking into account the first (1) and the last (2) runs in zero field measured at temperatures up to about

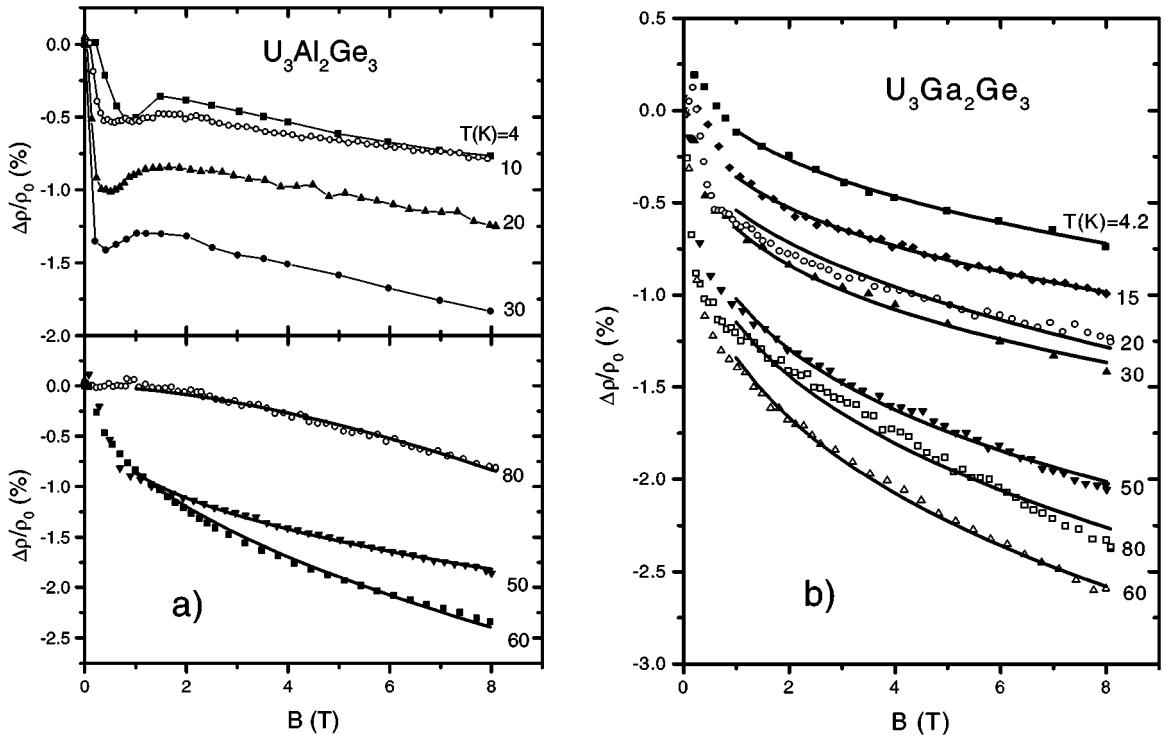

FIG. 7. The magnetoresistivity $\Delta\rho/\rho_o$ as a function of an applied magnetic field for (a) $U_3Al_2Ge_3$ and (b) $U_3Ga_2Ge_3$ at various temperatures. The thick solid lines are fits described in text.

100 K, i.e., about 40 K below to reach T_C. It is worth noting in this figure that the two different MR variations below T_C, i.e., (3–1) and (3–2), join each other just at T_C. A clearer transition at T_t, being slightly shifted in a magnetic field of 8 T to higher temperature, is better marked just for the (3–1) curve, for which the low-temperature MR is even positive. On the other hand, the MR data taken from Fig. 7a for 8 T (solid circles) follow very well the curve (3–2), except the one point at 50 K, which matches better to the curve (3–1). As one could expect, all the data in the paramagnetic state follow only one curve.

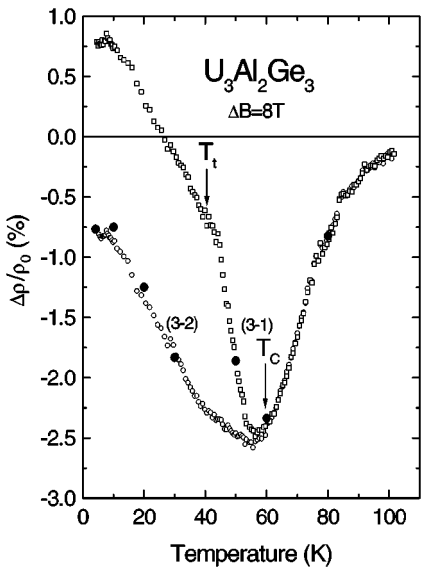

FIG. 8. The magnetoresistivity $\Delta\rho/\rho_o$ as a function of temperature for $U_3Al_2Ge_3$ taken in two runs (see text). The solid circles represent the data from Fig. 7a at 8 T.

In turn, the $\Delta\rho/\rho_o$ vs B dependence for $U_3Ga_2Ge_3$ is plotted in Fig. 7b. Also for this compound MR is negative, except for some low-field range at 4.2 K, where a slight positive behavior is noted. Because measurements were made only up to about 100 K (i.e., near T_C), all the curves presented in Fig. 7b concern solely the ordered state. As mentioned earlier in describing the zero-field $\rho(T)$ curve, we expect for this germanide the presence of an additional transition at $T_t = 63$ K, which has not yet been discovered by neutron diffraction (4). One sees in this figure that all the curves taken from 4.2 to 100 K behave in a similar fashion, without a distinct change of the character around T_t, as was the case of the Al-containing germanide, and show in all this range of temperatures an—AB^n dependence ($n \approx 0.3$–0.5), with a small tendency to saturation at higher fields. The MR values obtained at 8 T at various temperatures (solid squares) are also plotted in Fig. 9 together with the two $\Delta\rho/\rho_o$ vs T curves obtained by subtraction of the zero-field curves (1) and (3) (see Fig. 6b) from that determined in an applied magnetic field of 8 T (curve 4). Inspecting Fig. 9, one sees the closeness in the character of both the curves (4–1)

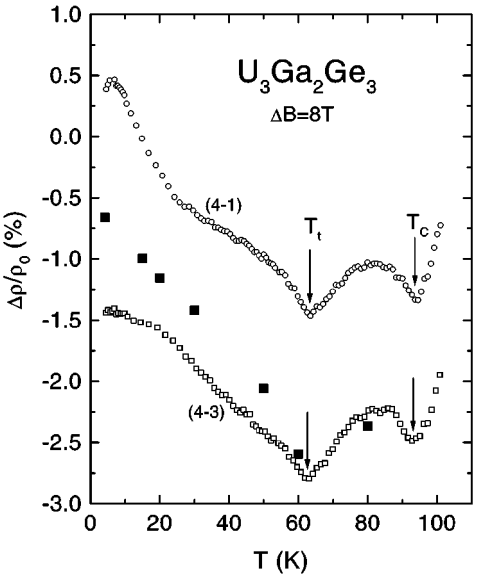

FIG. 9. The magnetoresistivity $\Delta\rho/\rho_o$ as a function of temperature for $U_3Ga_2Ge_3$ taken in two runs (see text). The solid squares represent the data from Fig. 7b at 8 T.

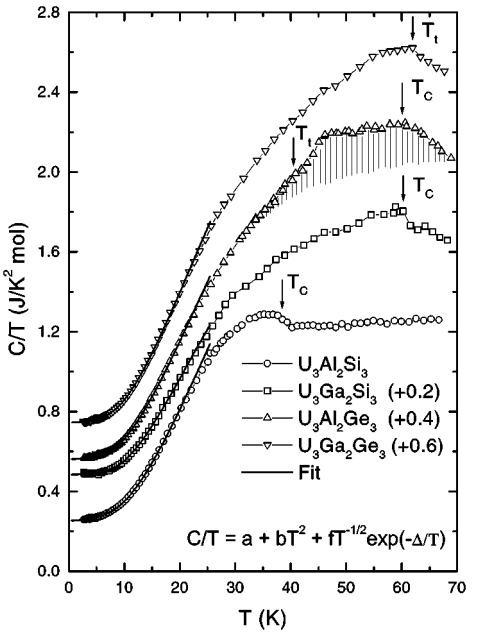

FIG. 10. C/T vs T plot for $U_3(Al,Ga)_2(Si,Ge)_3$. The solid line is a fit to the expression shown in the figure. The corresponding parameters are presented in Table 2. The parameter a corresponds to the electronic specific heat coefficient $\gamma(0)$.

and (4–3). They are, however, shifted from each other. Also, the experimental points obtained from the field-dependent MR at 8 T (Fig. 7b) are located between these two curves. Nevertheless, the most important fact emerging from the character of all these curves is the existence of a clear transition at T_t, where MR takes the highest negative value, while this quantity at T_C is slightly lower in an absolute value. As is demonstrated in the upper inset of Fig. 6b, where the temperature dependent derivatives of the resistivity in zero field and at 8 T are displayed, the T_t and T_C transitions, taken in this case at the respective inflection points due to the ferromagnetic properties of these materials, may change negligibly with the application of a magnetic field as high as 8 T.

The presence of the transition at $T_t = 63$ K in $U_3Ga_2Ge_3$ is also confirmed by the heat capacity measurements described below. However, we hope that any further accurate neutron diffraction studies, e.g., on single-crystalline samples of this compound, may confirm such a transition.

3.3. Heat Capacity

Figure 10 presents the specific heat C_p divided by T, measured in the temperature range 2–70 K for all four intermetallics. Small but distinct anomalies are observed at the transition temperatures T_t and T_C marked by respective arrows. For $U_3Al_2Ge_3$ the transitions at T_t and T_C form together a wide hump giving rise to a "speculation" that the sine-wave modulated propagation vector changes with temperature up to T_C. For $U_3Ga_2Ge_3$ we were able only to detect the transition at $T_t = 63$ K due to the limitation in the temperature range of measurements. The presence of this transition in the specific heat data confirms the anomalies occurring at this temperature in other measurements presented above. The solid lines in Fig. 10 represent the least-squares fits according to the anisotropic model reported by Andersen and Smith (13). This model introduces the gap Δ in the dispersion relation of magnons for the materials exhibiting an easy plane anisotropy (see the expression in Fig. 10). The parameters obtained are gathered in Table 2. The C/T values at 2 K (parameter a in the equation) are enhanced, especially for silicides. The values of the gap Δ, on the order of 50 K, are reasonable and comprise the range; they are close to those found from the electrical resistivity measurements.

TABLE 2
C_p Data Fitted to the Equation of Andersen and Smith[a]

Compound	a J/K^{2}mol	b 10^{-4} J/K^{4}mol	f J/K$^{3/2}$mol	Δ (K)
$U_3Al_2Si_3$	0.253(1)	7.0(2)	17.9(5)	54(1)
$U_3Ga_2Si_3$	0.284(1)	3.0(1)	21.1(6)	52(1)
$U_3Al_2Ge_3$	0.161(1)	6.0(2)	18.2(4)	49.3(5)
$U_3Ga_2Ge_3$	0.145(1)	6.0(3)	20.3(5)	48.5(5)

[a] *Phys. Rev. B* **19,** 384 (1979).

ACKNOWLEDGMENTS

This work was supported by the State Committee for Scientific Research (KBN) under Grant 2PO3B 150 17. The authors are furthermore grateful to the Austrian–Polish Scientific Technical Exchange Program. The authors also thank Mr. D Badurski for his technical assistance.

REFERENCES

1. F. Weitzer, M. Potel, H. Noël, and P. Rogl, *J. Solid State Chem.* **111,** 267 (1994).
2. P. Rogl, G. André, F. Weitzer, M. Potel, and H. Noël, *J. Solid State Chem.* **131,** 72 (1997).
3. P. Rogl, G. André, F. Bourée, and H. Noël, *J. Magn. Magn. Mater.* **191,** 291 (1999).
4. M. Mihalik, P. Rogl, and A. A. Menovsky, *Physica B* **259**/**261,** 258 (1999).
5. R. Troć, V. Zaremba, M. Kuzniec, and Y. Levin, *J. Alloys Compd.* **297,** 9 (2000).
6. R. J. Elliott and F. A. Wedgwood, *Proc. Phys. Soc.* **81,** 846 (1963). H. R. Ott, H. Rudiger, E. Felder, Z. Fisk, and B. Batlogg, *Phys. Rev. Lett.* **55,** 1595 (1985).
7. P. Pechev, B. Chevalier, D. Laffargue, B. Darriet, T. Roisnel, and J. Etourneau, *J. Magn. Magn. Mater.* **191,** 282 (1999).
8. J. Schoenes, B. Frick, and O. Vogt, *Phys. Rev. B* **30,** 6578 (1984).
9. A. Bernasconi, M. Mombelli, Z. Fisk, and H. R. Ott, *Z. Phys. B* **94,** 423 (1994).
10. E. Fawcett, *Rev. Mod. Phys.* **60,** 209 (1988).
11. H. Yamada and S. Takada, *J. Phys. Soc. Jpn.* **34,** 51 (1973).
12. B. Chevalier, J. Garcia Soldevilla, J. I. Espeso, J. Rodriguez Fernandez, J. C. Gomez Sal, and J. Etourneau, *Physica B* **259/261,** 44 (1999).
13. N. H. Andersen and H. Smith, *Phys. Rev. B* **19,** 384 (1979).